Electronic Supplementary Material (ESI) for New Journal of Chemistry.

Three Novel Indole-Bearing Porous Organic Polymers for Efficient Iodine Capture from Both Vapor and Organic Phases

Jingwen Yu[a,b], Luna Song[c], Yeshuang Wang[a], Haowen Li[d], Jiawen Liu[a], Mengmeng Wu[a,*], Yu Feng[a], and Jie Mi[a,*]

[a] *State Key Laboratory of Clean and Efficient Coal Utilization/Key Laboratory of Coal Science and Technology of Shanxi Province and Ministry of Education, Taiyuan University of Technology, Taiyuan, China 030024, China, E-mail: mijie111@163.com, wumengmeng111@126.com.*

[b] *Lu'an Chemical Group Co., Ltd., Changzhi 046204, China*

[c] *Shanxi Institute of Energy, Jinzhong 030600, China*

[d] *College of Textile Engineering, Taiyuan University of Technology, Taiyuan 030600, China*

Table of Contents

1. FT-IR details of Ph-TIn

Table S1. Analysis of characteristic peaks of Ph-TIn.

Wave number (cm^{-1})	Vibrational mode of characteristic group
3453	N-H stretching vibration on indole ring
3423	O-H stretching vibration of water coming from KBr
3035	C-H stretching vibration of aromatic ring (indole ring and benzene ring)
2850	C-H stretching vibration of methyne
1616, 1503, 1455	Skeleton stretching vibration of aromatic ring (indole ring and benzene ring)
1342	C-H bending vibration of methyne
745 (strong)	C-H bending vibration of four adjacent hydrogen atoms on the indole ring (benzo)

2. X-ray diffraction details of Ph-TIn

Table S2. Crystal structure parameters of Ph-TIn.

Chemical formula	$C_{40}H_{30}N_4$
Formula weight	566.68
Temperature/K	150.00
Color, habit	Colourless, Block
Crystal size/mm^3	0.12 × 0.11 × 0.10
Crystal system	triclinic
Space group	P-1
a/Å	11.2613(5)
b/Å	12.2335(5)
c/Å	14.3259(6)
α/°	66.0230(10)
β/°	78.933(2)
γ/°	67.3370(10)
Volume/Å^3	1662.60(12)
Z	2
Calculated density g/cm^{-3}	1.132
Absorption coefficient/mm^{-1}	0.067
F(000)	596.0
Radiation	MoKα (λ = 0.71073)
2θ range for data collection/°	3.984 to 52.812
Index ranges	-14≤h≤14, -14≤k≤15, -17≤l≤ 17
Reflections collected	22987
Independent reflections	6782 [R_{int} = 0.0373, R_{sigma} = 0.0395]
Data/restraints/parameters	6782/0/397
Goodness-of-fit on F^2	1.042
Final R indices [I>2σ(I)]	R_1 = 0.0413, wR_2 = 0.1089
CCDC number	2189408

Table S3. Bond lengths [Å] for Ph-TIn.

Atom-Atom	Length	Atom-Atom	Length
N1-C11	1.3785(14)	C16-C17	1.3851(17)
N1-C13	1.3717(15)	C18-C19	1.3953(15)
N2-C7	1.3747(16)	C18-C23	1.3891(15)
N2-C8	1.3817(15)	C19-C20	1.3836(16)
N3-C34	1.3770(16)	C20-C21	1.3940(16)
N3-C35	1.3768(16)	C21-C22	1.3853(16)
N4-C26	1.3797(17)	C21-C24	1.5235(15)
N4-C27	1.3732(16)	C22-C23	1.3895(16)
C1-C2	1.4409(15)	C24-C25	1.5120(16)
C1-C8	1.3648(16)	C24-C33	1.5129(15)
C1-C9	1.5123(15)	C25-C26	1.3585(17)
C2-C3	1.4040(16)	C25-C28	1.4397(15)
C2-C7	1.4160(16)	C27-C28	1.4116(17)
C3-C4	1.3847(17)	C27-C32	1.3947(17)
C4-C5	1.4047(19)	C28-C29	1.4016(16)
C5-C6	1.379(2)	C29-C30	1.3839(17)
C6-C7	1.3985(17)	C30-C31	1.400(2)
C9-C10	1.5124(14)	C31-C32	1.3767(19)
C9-C18	1.5227(14)	C33-C34	1.3665(16)
C10-C11	1.3669(16)	C33-C40	1.4412(15)
C10-C12	1.4396(15)	C35-C36	1.3946(17)
C12-C13	1.4174(15)	C35-C40	1.4155(16)
C12-C17	1.4031(16)	C36-C37	1.3788(19)
C13-C14	1.4010(16)	C37-C38	1.4053(18)
C14-C15	1.3805(19)	C38-C39	1.3836(17)
C15-C16	1.4055(19)	C39-C40	1.4046(16)

Table S4. Bond angles [Å] for Ph-TIn.

Atom-Atom-Atom	Angle	Atom-Atom-Atom	Angle	Atom-Atom-Atom	Angle
C13-N1-C11	109.44(9)	C17-C12-C10	134.09(10)	N4-C27-C28	107.06(10)
C7-N2-C8	108.54(10)	C17-C12-C13	118.97(10)	N4-C27-C32	130.66(12)
C35-N3-C34	108.72(10)	N1-C13-C12	107.24(10)	C32-C27-C28	122.27(11)
C27-N4-C26	109.07(10)	N1-C13-C14	130.71(11)	C27-C28-C25	107.35(10)
C2-C1-C9	125.32(10)	C14-C13-C12	122.03(11)	C29-C28-C25	133.80(11)
C8-C1-C2	106.18(10)	C15-C14-C13	117.26(11)	C29-C28-C27	118.84(11)
C8-C1-C9	128.39(10)	C14-C15-C16	121.89(11)	C30-C29-C28	118.81(12)
C3-C2-C1	133.88(11)	C17-C16-C15	120.64(12)	C29-C30-C31	121.19(12)
C3-C2-C7	119.02(10)	C16-C17-C12	119.18(11)	C32-C31-C30	121.33(12)
C7-C2-C1	107.08(10)	C19-C18-C9	121.15(9)	C31-C32-C27	117.52(12)
C4-C3-C2	118.96(11)	C23-C18-C9	120.80(10)	C34-C33-C24	127.64(10)
C3-C4-C5	120.96(12)	C23-C18-C19	118.04(10)	C34-C33-C40	106.12(10)
C6-C5-C4	121.45(11)	C20-C19-C18	120.77(10)	C40-C33-C24	126.24(10)
C5-C6-C7	117.67(12)	C19-C20-C21	121.13(10)	C33-C34-N3	110.53(11)
N2-C7-C2	107.65(10)	C20-C21-C24	120.83(10)	N3-C35-C36	130.52(11)
N2-C7-C6	130.44(11)	C22-C21-C20	118.04(10)	N3-C35-C40	107.48(10)
C6-C7-C2	121.90(11)	C22-C21-C24	121.12(10)	C36-C35-C40	122.00(11)
C1-C8-N2	110.54(10)	C21-C22-C23	120.99(10)	C37-C36-C35	117.85(12)
C1-C9-C10	113.13(9)	C18-C23-C22	121.00(10)	C36-C37-C38	121.21(11)
C1-C9-C18	111.96(9)	C25-C24-C21	110.70(9)	C39-C38-C37	121.06(11)
C10-C9-C18	111.49(8)	C25-C24-C33	112.11(9)	C38-C39-C40	118.97(11)
C11-C10-C9	128.00(10)	C33-C24-C21	111.40(9)	C35-C40-C33	107.14(10)
C11-C10-C12	106.67(9)	C26-C25-C24	128.61(11)	C39-C40-C33	133.96(10)
C12-C10-C9	125.26(10)	C26-C25-C28	106.28(10)	C39-C40-C35	118.90(10)
C10-C11-N1	109.68(10)	C28-C25-C24	125.10(10)		
C13-C12-C10	106.92(10)	C25-C26-N4	110.17(11)		

Table S5. Fractional atomic coordinates ($\times 10^4$) and equivalent isotropic displacement parameters ($Å^2 \times 10^3$) for Ph-TIn.

Atom	x	y	z	U(eq)
N1	4484(1)	6452.2(9)	9272.0(7)	25.9(2)
N2	8037.2(10)	3020.1(10)	7056.5(8)	29.6(2)
N3	2016.9(11)	12127.1(10)	3828.3(8)	33.5(2)
N4	7323.6(11)	10176.9(10)	2151.0(9)	38.3(3)
C1	5997.5(11)	4223.6(10)	7317.4(8)	21.5(2)
C2	6260.7(11)	2961.2(10)	8086.2(8)	21.9(2)
C3	5532.6(11)	2374.1(11)	8908.5(9)	25.1(2)
C4	6089.9(13)	1102.9(12)	9506.1(9)	31.0(3)
C5	7351.8(13)	394.6(12)	9284(1)	33.8(3)
C6	8088.2(12)	941.3(11)	8477.5(10)	31.2(3)
C7	7539.7(11)	2234.0(11)	7890.1(9)	25.8(2)
C8	7098.2(11)	4209.8(11)	6717.1(9)	26.9(2)
C9	4714.4(10)	5295.4(10)	7189.2(8)	19.7(2)
C10	4370.4(10)	5817(1)	8036.0(8)	20.0(2)
C11	5187.0(11)	5848.9(11)	8610.3(8)	23.9(2)
C12	3082.4(11)	6446.6(10)	8352.1(8)	21.0(2)
C13	3194.4(11)	6804.6(10)	9147.3(8)	22.6(2)
C14	2113.4(12)	7431.1(11)	9642.0(9)	28.1(3)
C15	920.2(12)	7728.2(12)	9302(1)	31.9(3)
C16	782.0(12)	7404.9(12)	8502.8(10)	33.3(3)
C17	1852.4(11)	6762.9(11)	8029.7(9)	27.5(2)
C18	4630.9(10)	6350.3(10)	6139.6(8)	19.9(2)
C19	5224.5(11)	7245.6(11)	5917.0(8)	24.0(2)
C20	5152.9(11)	8194.5(11)	4958.5(9)	24.8(2)

C21	4465.8(11)	8300.7(10)	4195.2(8)	21.8(2)
C22	3888.5(12)	7403.3(11)	4413.4(9)	28.5(3)
C23	3975.5(12)	6436.6(11)	5369.8(9)	27.8(3)
C24	4335.5(11)	9387(1)	3159.1(8)	22.8(2)
C25	5636.7(11)	9496(1)	2723.2(8)	23.9(2)
C26	6061.8(13)	10471.8(12)	2522.7(10)	33.3(3)
C27	7722.8(12)	9005.3(11)	2071.7(9)	27.6(3)
C28	6692.6(11)	8533.7(10)	2448.6(8)	22.9(2)
C29	6859.3(12)	7323.8(11)	2479.1(9)	28.1(3)
C30	8015.4(13)	6649.1(12)	2111.7(11)	35.8(3)
C31	9012.0(13)	7151.3(12)	1720.3(10)	36.8(3)
C32	8886.1(12)	8326.2(12)	1698.6(10)	33.6(3)
C33	3376.2(11)	10627.6(11)	3222.0(8)	23.6(2)
C34	2838.4(12)	10884.0(12)	4082.8(9)	29.3(3)
C35	2003.8(12)	12703.5(11)	2779.1(9)	27.7(3)
C36	1327.1(13)	13941.6(12)	2155.5(11)	35.0(3)
C37	1489.2(13)	14254.0(12)	1111.4(10)	34.2(3)
C38	2309.6(12)	13356.4(12)	686.7(9)	30.7(3)
C39	2991.1(11)	12130.8(11)	1303.3(9)	26.2(2)
C40	2844.6(11)	11785.7(10)	2369.8(9)	23.0(2)

Table S6. Anisotropic displacement parameters ($Å^2 \times 10^3$) for Ph-TIn.

Atom	U11	U22	U33	U23	U13	U12
N1	31.7(5)	28.5(5)	21.1(5)	-11.6(4)	-3.6(4)	-10.2(4)
N2	24.6(5)	28.5(5)	30.2(5)	-11.2(4)	0.9(4)	-3.9(4)
N3	36.8(6)	30.9(6)	28.0(5)	-16.2(5)	-2.2(4)	-0.5(5)
N4	40.0(6)	23.0(5)	49.5(7)	-11.0(5)	13.1(5)	-17.8(5)
C1	26.1(6)	20.2(5)	19.0(5)	-8.0(4)	-2.7(4)	-7.1(4)
C2	26.2(6)	21.0(5)	20.1(5)	-8.6(4)	-5.9(4)	-6.3(4)
C3	29.1(6)	24.5(6)	23.9(5)	-8.6(5)	-4.6(4)	-10.0(5)
C4	39.8(7)	26.4(6)	27.4(6)	-3.8(5)	-8.2(5)	-15.3(5)
C5	43.0(7)	19.7(6)	35.9(7)	-4.1(5)	-18.0(6)	-6.8(5)
C6	30.2(6)	24.2(6)	37.6(7)	-11.9(5)	-11.7(5)	-2.0(5)
C7	27.4(6)	24.9(6)	25.9(6)	-10.8(5)	-6.7(4)	-5.8(5)
C8	29.2(6)	23.9(6)	24.0(6)	-7.6(5)	-0.1(4)	-7.1(5)
C9	23.5(5)	18.0(5)	18.3(5)	-6.3(4)	-1.4(4)	-7.9(4)
C10	25.2(5)	16.4(5)	16.1(5)	-3.8(4)	-0.7(4)	-7.3(4)
C11	26.7(6)	23.1(5)	20.8(5)	-7.4(4)	-1.3(4)	-7.8(4)
C12	26.9(6)	16.6(5)	18.7(5)	-4.6(4)	-0.1(4)	-9.1(4)
C13	30.3(6)	18.2(5)	17.7(5)	-3.7(4)	0.1(4)	-10.4(4)
C14	38.8(7)	22.2(6)	20.9(5)	-8.1(4)	5.1(5)	-10.8(5)
C15	32.0(6)	24.4(6)	31.4(6)	-9.3(5)	9.8(5)	-7.9(5)
C16	25.3(6)	31.6(7)	39.3(7)	-10.5(5)	0.1(5)	-9.3(5)
C17	27.6(6)	27.3(6)	30.2(6)	-11.6(5)	-2.5(5)	-10.2(5)
C18	23.6(5)	17.1(5)	18.3(5)	-6.9(4)	-0.7(4)	-5.9(4)
C19	29.5(6)	24.3(6)	21.4(5)	-7.8(4)	-4.2(4)	-11.7(5)
C20	31.9(6)	22.6(6)	23.3(5)	-6.4(4)	-2.0(4)	-14.7(5)
C21	26.4(5)	18.7(5)	18.6(5)	-6.3(4)	-0.3(4)	-6.8(4)

C22	41.3(7)	27.6(6)	21.1(5)	-4.9(5)	-8.9(5)	-17.2(5)
C23	39.9(7)	24.3(6)	24.4(6)	-5.0(5)	-6.5(5)	-18.2(5)
C24	28.3(6)	18.2(5)	19.0(5)	-5.1(4)	-1.1(4)	-6.8(4)
C25	30.1(6)	17.6(5)	18.4(5)	-3.4(4)	-0.4(4)	-6.2(4)
C26	38.1(7)	19.7(6)	36.7(7)	-8.9(5)	9.1(5)	-11.0(5)
C27	31.7(6)	20.4(6)	23.0(5)	-1.6(4)	-0.7(5)	-8.1(5)
C28	27.3(6)	19.4(5)	17.1(5)	-3.2(4)	-4.2(4)	-5.2(4)
C29	30.7(6)	23.6(6)	30.4(6)	-10.6(5)	-4.3(5)	-7.5(5)
C30	38.4(7)	24.4(6)	40.8(7)	-14.8(5)	-3.2(6)	-3.3(5)
C31	30.8(7)	28.4(6)	35.1(7)	-8.7(5)	1.7(5)	1.9(5)
C32	28.6(6)	29.2(6)	29.9(6)	-1.9(5)	0.8(5)	-6.8(5)
C33	27.0(6)	21.2(5)	21.0(5)	-6.2(4)	-1.1(4)	-8.1(4)
C34	33.1(6)	27.6(6)	22.5(6)	-8.9(5)	-2.0(5)	-5.5(5)
C35	28.8(6)	25.9(6)	28.8(6)	-12.2(5)	-4.2(5)	-6.0(5)
C36	35.4(7)	24.0(6)	41.8(7)	-14.6(5)	-9.4(5)	0.0(5)
C37	35.6(7)	21.8(6)	38.6(7)	-3.8(5)	-12.5(5)	-5.6(5)
C38	33.6(6)	29.2(6)	25.5(6)	-3.5(5)	-4.7(5)	-12.2(5)
C39	27.7(6)	24.9(6)	24.5(6)	-7.6(5)	-0.7(4)	-9.1(5)
C40	23.8(5)	19.6(5)	25.0(6)	-7.4(4)	-1.8(4)	-7.2(4)

3. Preparation, porosity, and iodine adsorption performance of InPOPs

Preparation of Polymer-1： Under nitrogen atmosphere, Ph-TIn (566.3 mg, 1 mmol, 1 eq.) and a certain amount of anhydrous $FeCl_3$ were added into a dry 100 mL double-necked round-bottomed flask equipped with a magnetic stirrer and a condenser as soon as possible. Subsequently, anhydrous 1,2-dichloroethane (60 mL) was injected into the flask under nitrogen protection. After 10 min of stirring, FDA (the molar ratio of FDA to $FeCl_3$ was always kept 1:1[1-6]) was added dropwise to the aforementioned mixture. The mixture was stirred at 45 ℃ for 5 h to form an initial network, then refluxed at 80 ℃ for another 19 h to strengthen the network. After being cooled down to ambient temperature, the insoluble solid was obtained by filtration and subsequently washed with the recovered mixture of methanol and ethanol to remove unreacted monomers and $FeCl_3$ until the filtrate became colorless. The material was further purified by Soxhlet extraction with the recovered mixture of methanol and ethanol for 24 h and finally vacuum-dried at 90 °C for 24 h.

The obtained polymers with different FDA/Ph-TIn molar ratios of 6, 8, 10, and 12 are referred to as Polymer-1-1, -1-2, -1-3, and -1-4, respectively. The data of pore properties for the obtained polymers are summarized in Table S7. It is found that with the increase of FDA/Ph-TIn molar ratio, the BET specific surface area changes little and stabilizes at about 460 $m^2 g^{-1}$.

Table S7. Pore properties of polymers (FDA as crosslinker).

Dosages of FDA and $FeCl_3$	Material name	Specific surface area (S_{BET}, $m^2 g^{-1}$)	Pore volume (V, $cm^3 g^{-1}$)	Average pore size (nm)
FDA-6 eq; $FeCl_3$-6 eq	Polymer-1-1	468	0.396	3.383
FDA-8 eq; $FeCl_3$-8 eq	Polymer-1-2	455	0.409	3.593
FDA-10 eq; $FeCl_3$-10 eq	Polymer-1-3	455	0.374	3.292
FDA-12 eq; $FeCl_3$-12 eq	Polymer-1-4	456	0.363	3.181

Preparation of Polymer-2： Under nitrogen atmosphere, Ph-TIn (566.3 mg, 1 mmol, 1eq.), a certain amount of DCX and anhydrous $FeCl_3$ (the molar ratio of DCX to $FeCl_3$ was always kept 1:1[1,7]) were added into a dry 100 mL double-necked round-bottomed flask equipped with a magnetic stirrer and a condenser as soon as possible. Afterward, anhydrous 1,2-dichloroethane (60 mL) was

injected into the aforementioned mixture under a flow of nitrogen. The mixture was heated at 80 °C for 24 h at constant stirring. After cooling to room temperature, the precipitate was collected by filtration and successively washed by the recovered mixture of methanol and ethanol several times until the filtrate turned clear. Further purification of the polymer was carried out by Soxhlet extraction with the recovered mixture of methanol and ethanol for 24 h, and dried under vacuum at 90 °C for 24 h.

The obtained polymers with different DCX/Ph-TIn molar ratios of 4, 6, 8, and 10 are referred to as Polymer-2-1, -2-2, -2-3, and -2-4, respectively. The data of pore properties for the obtained polymers are summarized in Table S8. It is found that with the increase of DCX/Ph-TIn molar ratio, the BET surface area increases from 111 to 759 $m^2 g^{-1}$.

Table S8. Pore properties of polymers (DCX as crosslinker).

Dosages of DCX and $FeCl_3$	Material name	Specific surface area (S_{BET}, $m^2 g^{-1}$)	Pore volume (V, $cm^3 g^{-1}$)	Average pore size (nm)
DCX-4 eq; $FeCl_3$-4 eq	Polymer-2-1	111	0.197	7.079
DCX -6 eq; $FeCl_3$-6 eq	Polymer-2-2	539	0.393	2.919
DCX -8 eq; $FeCl_3$-8 eq	Polymer-2-3	661	0.465	2.813
DCX -10 eq; $FeCl_3$-10 eq	Polymer-2-4	759	0.501	2.644

Preparation of Polymer-3： Under nitrogen atmosphere, Ph-TIn (566.3 mg, 1 mmol, 1eq.) and a certain amount of anhydrous $FeCl_3$ were added into a dry 100 mL double-necked round-bottomed flask as soon as possible. Then, anhydrous 1,2-dichloroethane (60 mL) was injected into the aforementioned mixture under a flow of nitrogen. The reaction mixture was stirred at 80 °C for 24 h and left to cool to room temperature. The insoluble residue was filtered off and washed with the recovered mixture of methanol and ethanol until the filtrate became colorless. The filter cake was successively extracted with the recovered mixture of methanol and ethanol in a Soxhlet apparatus for 24 h, and then dried in a vacuum oven at 90 °C for 24 h. The obtained polymers with different $FeCl_3$/Ph-TIn molar ratios of 8, 10, 12, and 14 are referred to as Polymer-3-1, -3-2, -3-3, and -3-4, respectively. The data of pore properties for the obtained polymers are summarized in Table S9. It is

found that with the increase of $FeCl_3$/Ph-TIn molar ratio, the BET surface area increases from 40 to 135 $m^2 g^{-1}$.

Table S9. Pore properties of polymers (no crosslinker).

Dosage of $FeCl_3$	Material name	Specific surface area (S_{BET}, $m^2 g^{-1}$)	Pore volume (V, $cm^3 g^{-1}$)	Average pore size (nm)
$FeCl_3$-8 eq	Polymer-3-1	40	0.101	10.072
$FeCl_3$-10 eq	Polymer-3-2	52	0.120	9.217
$FeCl_3$-12 eq	Polymer-3-3	75	0.185	9.934
$FeCl_3$-14 eq	Polymer-3-4	135	0.285	8.419

The adsorption capacities of all obtained polymers toward iodine in organic phase were investigated. 5.0 mg of sorbent was immersed in an iodine/cyclohexane solution (20 mL, 200 mg L^{-1}) and allowed to stand for 48 h at 25 °C. Then, the supernatant was gauged by employing UV-Vis spectroscopy after adsorption. All materials participated in the adsorption procedure under the same conditions.

The data of iodine adsorption abilities for the obtained polymers are summarized in Fig. S1. It is found that polymer-1-3, polymer-2-2, and polymer-3-2 perform the best in their respective series. In what follows, we renamed the three polymers as InPOP-1, InPOP-2, and InPOP-3, respectively.

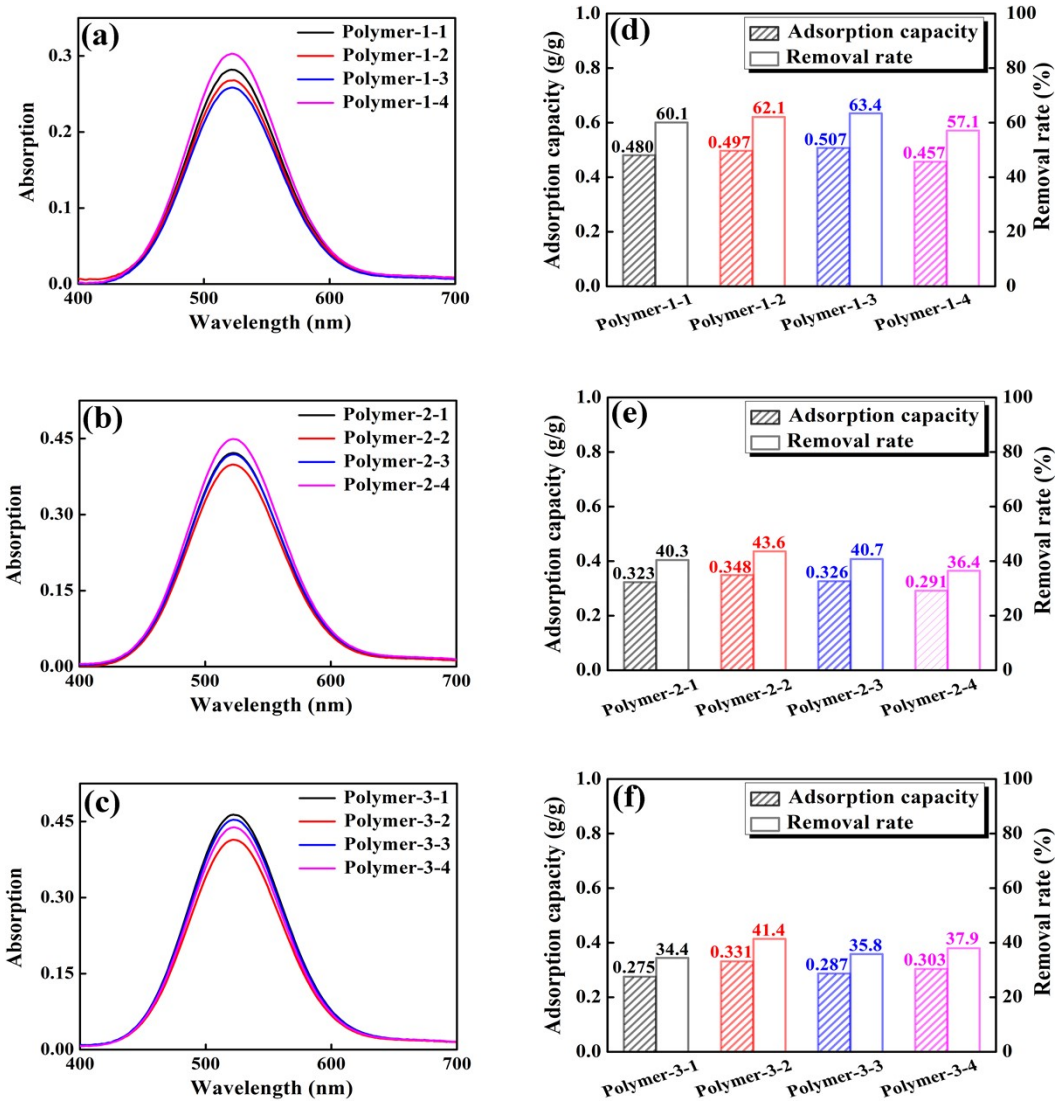

Fig. S1. (a-c) UV-Vis absorption spectra of iodine/cyclohexane solutions after adsorption by the obtained polymers under the same conditions and (d-f) the corresponding iodine adsorption capacitiy and removal rate.

4. FT-IR details of InPOPs

Table S10. Analysis of characteristic peaks of InPOP-1.

Wave number (cm^{-1})	Vibrational mode of characteristic group
3418	N-H stretching vibration on indole ring; O-H stretching vibration of water coming from KBr
2923, 2856	C-H stretching vibration of methylene
1610	Skeleton stretching vibration of aromatic ring (indole ring and benzene ring)
1450	Skeleton stretching vibration of aromatic ring (indole ring and benzene ring); C-H bending vibration of methylene
745 (weak)	C-H bending vibration of four adjacent hydrogen atoms on the indole ring (benzo)

Table S11. Analysis of characteristic peaks of InPOP-2.

Wave number (cm^{-1})	Vibrational mode of characteristic group
3429	N-H stretching vibration on indole ring; O-H stretching vibration of water coming from KBr
2923, 2850	C-H stretching vibration of methylene
1610, 1509	Skeleton stretching vibration of aromatic ring (indole ring and benzene ring)
745 (weak)	C-H bending vibration of four adjacent hydrogen atoms on the indole ring (benzo)

Table S12. Analysis of characteristic peaks of InPOP-3.

Wave number (cm^{-1})	Vibrational mode of characteristic group
3418	N-H stretching vibration on indole ring; O-H stretching vibration of water coming from KBr
2923	C-H stretching vibration of methyne
1610, 1455	Skeleton stretching vibration of aromatic ring (indole ring and benzene ring)
745 (strong)	C-H bending vibration of four adjacent hydrogen atoms on the indole ring (benzo)

5. Comparison of iodine adsorption capacities in vapor phase

Table S13. Summary of the iodine vapor adsorption capacity of various functionalized materials at 75 ℃ under ambient pressure.

	Material type	Material name	Adsorption capacity (g/g)	Ref.
Metal-containing materials	Bayberry tannin and nano-silver based on collagen fiber	Ag^0@BT-nCF	1.704	[8]
	Bi_2S_3@polyacrylonitrile Hybrid bead	Bi_2S_3@PAN-70%	0.986	[9]
	Cu-BTC@PES composite bead	Cu-BTC@PES	up to 0.639	[10]
	Layered double hydroxides (LDHs)	NiTi-S_x-LDH	0.526	[11]
		NiTi-CO_3-LDH	0.250	
		NiTi-NO_3-LDH	0.191	
		BiZnAl-LDH	up to 0.433	[12]
	Metal-organic frameworks (MOFs)	UiO-66	0.68	[13]
		UiO-66-BA-20	1.509	
		UiO-66-BA-35	1.610	
		UiO-66-BA-50	1.578	
		$[Zn_2(tptc)(apy)_{2-x}(H_2O)_x]\cdot H_2O$	2.16	[14]
	IL@MOF composite (IL stands for ionic liquid)	IL@PCN-333(Al)	7.35	[15]
	MOF@Polymer composite beads	HKUST-1@PES	0.376	[16]
		HKUST-1@PVDF	0.225	
		HKUST-1@PEI	0.348	
	Electrospun fiber adsorbents	N-MOF-PAN fibers	3.20	[17]
		MOF-PAN fibers	1.13	

Carbon materials	Hyperporous carbon	THPS-C	3.40	[18]
	Carbon fabrics	CC-PNP	1.02	[19]
		C60-CC-PNP	2.40	
	Activated charcoal	AC	2.46	This work
Porous organic polymers (POPs)	Organic cages	BPPOC	5.64	[20]
		BPy-Cage	3.23	[21]
	Porous silsesquioxane-imine frameworks	PSIF-1a	4.85	[22]
		PSIF-2a	3.46	
		PSIF-3a	4.11	
		PSIF-4a	2.44	
		PSIF-5a	3.01	
	Covalent organic frameworks (COFs)	USTB-1	4.45	[20]
		USTB-2	4.38	
		USTB-3	3.14	
		USTB-1c	5.80	
		USTB-2c	4.57	
		USTB-3c	3.30	
		SIOC-COF-7	4.81	[23]
	Covalent triazine frameworks (CTFs)	CTF-1@$ZnCl_2$	4.31	[24]
		CTF-1@$ZnCl_2$·H_2O	2.41	
		CTF-1@TFMS	1.18	
	BODIPY-based conjugated porous polymers	BDP-CPP-1	2.83	[25]
		BDP-CPP-2	2.23	
	Charged porous aromatic frameworks	PAF-23	2.71	[26]
		PAF-24	2.76	
		PAF-25	2.60	
	Thiophene-based hypercrosslinked polymer	S-HCP	3.60	[27]

Melamine-functionalized carbonyl-rich polymers	TPA-TPC-6MA	2.92	[28]
	TPA-TPC-8MA	4.11	
	TPA-TPC-10MA	5.05	
Adamantane-based porous organic polymers	NOP-54	2.02	[1]
	NOP-53	1.77	
	NOP-52	1.39	
Ferrocene-based porous organic polymer	FcTz-POP	3.96	[29]
Pitch-based porous polymer bead	PHCP@PES	up to 0.77	[30]
Carbazole-based porous organic polymers	CSU-CPOPs-1	4.94	[7]
	CSU-CPOPs-2	4.24	
	CSU-CPOPs-3	3.47	
	CTF-CAR	2.86	[31]
Indole-based porous organic polymers	InPOP-1	2.19	This work
	InPOP-2	1.92	
	InPOP-3	2.92	

6. Supporting references

[1] D. Y. Chen, Y. Fu, W. G. Yu, G. P. Yu, C. Y. Pan, *Chem. Eng. J.*, 2018, **334**, 900–906.

[2] T. Jin, S. H. An, X. J. Yang, J. Hu, H. L. Wang, H. L. Liu, Z. Q. Tian, D. E. Jiang, N. Mehio, X. Zhu, *Aiche J.*, 2016, **62**, 1740–1746.

[3] Y. T. Xia, Y. K. Li, Y. T. Gu, T. Jin, Q. Yang, J. Hu, H. L. Liu, H. L. Wang, *Fuel,* 2016, **170**, 100–106.

[4] C. Zhang, P. C. Zhu, L. X. Tan, J. M. Liu, B. E. Tan, X. L. Yang, H. B. Xu, *Macromolecules,* 2015, **48***,* 8509−8514.

[5] X. Zhu, S. M. Mahurin, S. H. An, C. Do-Thanh, C. C. Tian, Y. K Li, L. W. Gill, E. W. Hagaman, Z. J. Bian, J. H. Zhou, J. Hu, H. L. Liu, S. Dai, *Chem. Commun.,* 2014, **50**, 7933.

[6] B. Y. Li, R. N. Gong, W. Wang, X. Huang, W. Zhang, H. M. Li, C. X. Hu, B. E. Tan, *Macromolecules,* 2011, **44**, 2410–2414.

[7] S. H. Xiong, X. Tang, C. Y. Pan, L. Li, J. T. Tang, G. P. Yu, *ACS Appl. Mater. Interfaces.,* 2019, **11**, 27335−27342.

[8] B. Wang, H. Zhu, T. Duan, G. Q. He, Y. X. Wei, J. Zhou, *Appl. Surf. Sci.,* 2022, **596**, 153585.

[9] Q. Yu, X. H. Jiang, Z. J. Cheng, Y. W. Liao, Q. Pu, M. Duan, *New J. Chem.,* 2020, **44**, 16759–16768.

[10] Q. Zhao, L. Zhu, G. H. Lin, G. Y. Chen, B. Liu, L. Zhang, T. Duan, J. H. Lei, *ACS Appl. Mater. Interfaces.,* 2019, **11**, 42635−42645.

[11] G. H. Lin, L. Zhu, T. Duan, L. Zhang, B. Liu, J. H. Lei, *Chem. Eng. J.,* 2019, **378**, 122181.

[12] T. D. Dinh, D. X. Zhang, V. N. Tuan, *RSC Adv.,* 2020, **10**, 14360–14367.

[13] M. M. Jia, S. Y. Rong, P. C. Su, Li, W. B. Su, *Chem. Eng. J.,* 2022, **437**, 135432.

[14] R. X. Yao, X. Cui, X. X. Jia, F. Q. Zhang, X. M. Zhang, *Inorg. Chem.,* 2016, **55**, 9270−9275.

[15] Y. Z. Tang, H. L. Huang, J. Li, W. J. Xue, C. L. Zhong, *J. Mater. Chem. A,* 2019, **7**, 18324–18329.

[16] B. Valizadeh, T. N. Nguyen, B. Smit, K. C. Stylianou, *Adv. Funct. Mater.,* 2018, **28**, 1801596.

[17] D. Y. Chen, , T. T. Ma, X. Y. Zhao, X. F. Jing, R. Zhao, G. S. Zhu, *ACS Appl. Mater. Interfaces,* 2022, **14**, 47126−47135.

[18] Q. M. Zhang, T. L. Zhai, Z. Wang, G. Cheng, H. Ma, Q. P. Zhang, Y. H. Zhao, B. E. Tan, C. Zhang, *Adv. Mater. Interfaces,* 2019, **6**, 1900249.

[19] R. Muhammad, N. F. Attia, , S. Cho, J. Park, M. Jung, J. Chung, H. Oh, *Thin Solid Films,* 2020, **706**, 138049.

[20] C. Liu, Y. C. Jin, Z. H. Yu, L. Gong, H. L. Wang, , B. Q. Yu, W. Zhang, , J. Z. Jiang, *J. Am. Chem. Soc.,* 2022, **144**, 12390−12399.

[21] D. Luo, Y. L. He, J. Y. Tian, J. L. Sessler, X. D. Chi, *J. Am. Chem. Soc.,* 2022, **144**, 113−117.

[22] M. Janeta, W. Bury, S. Szafert, *ACS Appl. Mater. Interfaces,* 2018, **10**, 19964−19973.

[23] Z. J. Yin, , S. Q. Xu, T. G. Zhan, Q. Y. Qi, Z. Q. Wu, X. Zhao, *Chem. Commun.,* 2017, **53**, 7266–7269.

[24] X. M. He, S. Y. Zhang, X. Tang, S. H. Xiong, C. X. Ai, D. Y. Chen, J. T. Tang, C. Y. Pan, G. P. Yu, *Chem. Eng. J.,* **2019**, *371*, 314–318.

[25] Y. L. Zhu, Y. J. Ji, D. G. Wang, Y. Zhang, H. Tang, X. R. Jia, M. Song, G. P. Yu, G. C. Kuang, *J. Mater. Chem. A,* **2017**, *5*, 6622–6629.

[26] Z. J. Yan, Y. Yuan, Y. Y. Tian, D. M. Zhang, G. S. Zhu, *Angew. Chem. Int. Ed.,* **2015**, *54*, 12733–12737.

[27] X. M. Li, G. Chen, H. Xu, Q. Jia, *Sep. Purif. Technol.,* **2019**, *228*, 115739.

[28] D. Zhang, Y. P. Chen, J. J. Wang, Y. Wang, Y. W. Cao, J. W. Li, F. Zhou, J. H. Huang, Y. N. Liu, *Chem. Eng. J.,* **2023**, *460*, 141669.

[29] Y. Wang, J. Tao, S. H. Xiong, P. G. Lu, J. T. Tang, J. Q. He, M. U. Javaid, C. Y. Pan, G. P. Yu, *Chem. Eng. J.,* **2020**, *380*, 122420.

[30] G. Y. Chen, Q. Zhao, Z. R. Wang, M. Jiang, L. Zhang, T. Duan, L. Zhu, *J. Hazard. Mater.,* **2022**, *434*, 128859.

[31] H. Y. Wang, N. Qiu, X. F. Kong, Z. G. Hu, F. X. Zhong, Y. S. Li, H. J. Tan, *ACS Appl. Mater. Inter.,* **2023**, *15*, 14846–14853.